PWM Filter for Active Magnetic Bearings

Alexei Filatov[a] and Larry Hawkins[a]
a Calnetix Technologies
16323 Shoemaker Av., Cerritos, CA, 90703 USA, afilatov@calnetix.com, lhawkins@calnetix.com

Abstract

An example of a PWM filter application in an AMB amplifier is discussed. The design objectives included reduction of both conductive and radiated EMI caused by the PWM pulses, improving system efficiency, reliability, and enabling its use with long AMB cables. The selected filter topology included a "Trap" filter, utilizing a parallel LC resonant circuit to suppress output current harmonics near the circuit resonance, followed by a conventional 2nd-order LCR filter. This choice was dictated by a narrow frequency separation between the 25kHz PWM frequency in the existing amplifier and the required 2kHz bandwidth. Introduction of the filter resulted in the attenuation of the PWM signal at the base frequency ranging from -33.2dB to -52.7dB depending on the output current, which was varying from 0A to 10A. The filter practically eliminated high-frequency resonant ringing on the amplifier output and reduced output voltage dV/dt by more than 800 times (from 8,360V/μs to approximately 10 V/μs). Both factors are known to cause EMI and shorten the lives of the actuator magnet wires and the power electronics. The filter enabled the control current delivery to the AMB actuators in a commercial 350kW 15kRPM air compressor over 1.2 km (4,000 ft) cable. The compressor was subsequently levitated and spun to full speed.

Keywords: *Active Magnetic Bearings, PWM Filter, Switching Amplifier, EMI, Long Cable.*

1. Introduction

Active Magnetic Bearings (AMBs) typically use amplifiers with Pulse Width Modulation (PWM), which is the most common type of switching amplifiers that can be found anywhere from audio equipment to motor drives. While there are no practical alternatives to switching amplifiers because of their superior efficiency, they may also create problems when used without output filters. These include:

1. Electrical ground noises caused by high dV/dt associated with the edges of PWM pulses. These noises may affect the operation of other equipment on the same ground, for example the AMB position sensors (W. Santiago, 2004).
2. Radiated electromagnetic emissions due to
   a. Ripple currents.
   b. High-frequency resonant currents flowing in lightly damped LC-loops formed by the load and/or parasitic inductances in tandem with parasitic capacitances and excited by high-frequency content of PWM signals.
3. Reduced lives of actuator magnet wires and power electronics due to voltage spikes (Essex-Furukawa, 2020).
4. Increased eddy currents and hysteresis losses in the lamination stacks.
5. Difficulties of working with long cables (often this would be impossible without a PWM filter). (Essex-Furukawa, 2020) and (A. von Jouanne, et al., 1996).

2. PWM filter design

The PWM filter presented here is designed to work with an existing Calnetix mid-range amplifier which has a 25kHz switching frequency. Considering that many AMB applications require at least 2kHz control bandwidth, the separation between the upper limit of the control bandwidth and the amplifier switching frequency is only 23kHz. To maximize the attenuation of the PWM frequency without affecting the gains and phases of the system transfer functions within the control bandwidth, a filter topology described in (Y. Sozer et al., 2000) was selected. As shown in Fig.1, it consists of a "Trap filter", using a parallel LC resonant circuit to suppress output current harmonics with frequencies near the circuit resonance, followed by a conventional 2nd-order LCR filter. Because of the manufacturing tolerances on the inductances L_t, the trap filter is tuned by adjusting the filter capacitance C_t to closely match the resonant frequency to the amplifier switching frequency. This is a one-time adjustment that is independent of the load dynamics. In addition to the manufacturing tolerances, the current through the inductor also affects the inductance, causing the filter effectiveness

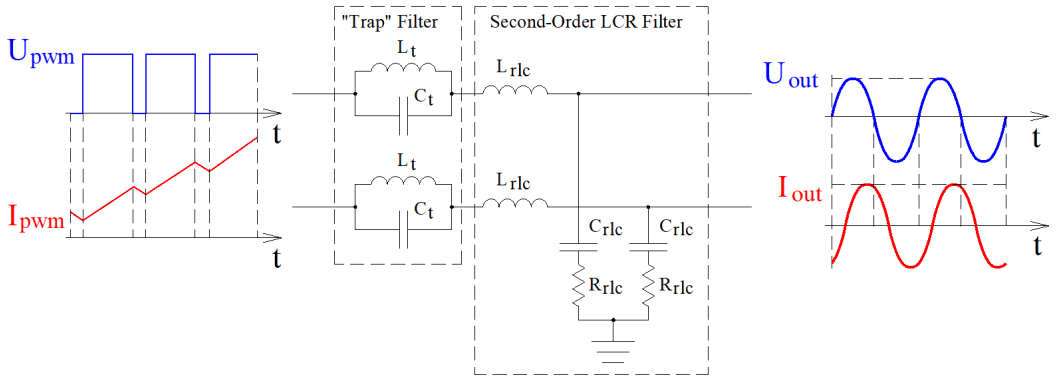

Figure 1. Topology of the PWM Filter.

to be dependent on this current level. Because the amplifier used for testing was rated for 10A continuous current with a typical load consuming less than 5A, the trap filter was tuned for the maximum effectiveness at 5A (-57dB theoretical best-case attenuation at 25kHz). For comparison, a 2nd-order LCR filter alone would yield only -9dB at 25 kHz. However, this simpler "LCR filter only" design would be less sensitive to the current level.

The PWM filter package includes an amplifier current feedback sensor as shown in Fig. 2, which is used in-lieu of the sensor in the standard location at the amplifier output. This allows the output current to follow the commanded current despite the filter dynamics.

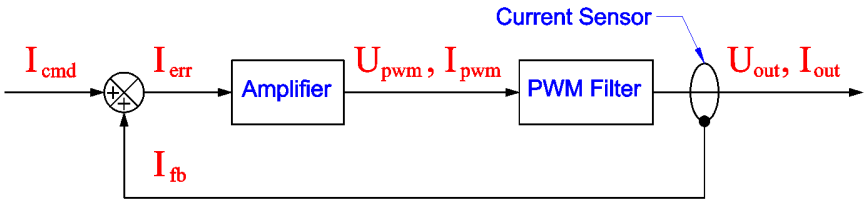

Figure 2. Integration of the PWM Filter into the Amplifier.

Fig. 3 shows a comparison of the voltage transfer functions of a combination "Trap + LCR" filter and a single LCR filter. The main advantage of the "Trap+LCR" filter is a much stronger attenuation of the PWM fundamental frequency, whereas the higher order harmonics, especially the second and the third, are attenuated somewhat less. The difference in the attenuation becomes nearly undistinguishable staring with the fourth harmonic. Stronger attenuation of the fundamental frequency by the "Trap+LCR" filter is very important, because this harmonic is dominant and largely responsible, for example, for the current ripple.

Fig. 4 shows comparison of the first three PWM harmonic amplitudes in the unfiltered voltage (a), after the LCR filter (b) and after the combination "Trap + LCR" filter (c) as functions of PWM duty cycles. When generating the curves shown

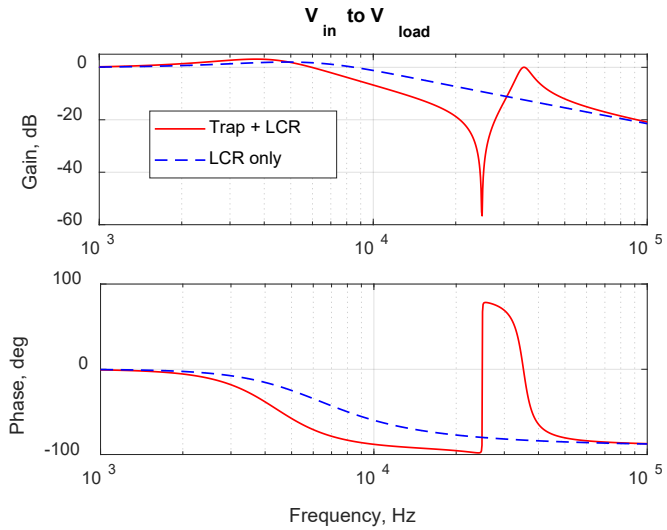

Figure 3. Comparison of the "Trap +LCR" and "LCR only" filter voltage transfer functions.

in Fig. 4, the amplitudes a_n of the PWM harmonics were calculated using equation (1) from (S.W. Smith, 1997):

$$a_n = \frac{2A}{n\pi}\sin(n\pi d) \quad (1)$$

where A is the PWM voltage, n is the harmonic number (n>0), and d is the duty cycle.

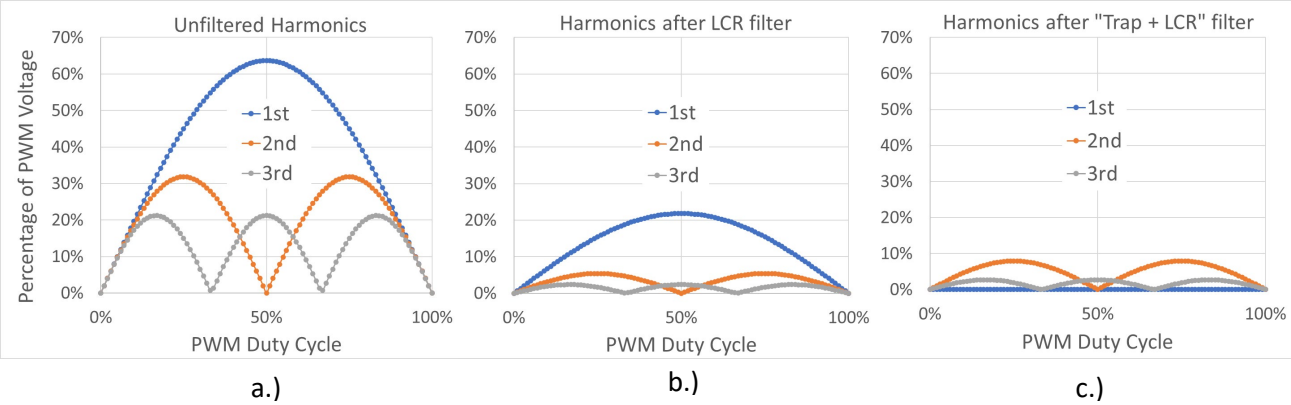

Figure 4. The first three voltage harmonic amplitudes as functions of PWM duty cycles without a filter (a), after the LCR filter (b), after the "Trap+LCR" filter (c).

3. Experimental setup

Fig. 5 shows the experimental setup used to tune the PWM filter and evaluate its performance on a bench. A standard production Magnetic Bearing Control (MBC) box incorporating an amplifier, a control board and a 200V amplifier power supply was used for the testing. The MBC in this setup had only five control channels because it was configured for a machine with all five degrees of freedom controlled by permanent-magnet-biased AMBs (no amplifier bias channels were needed). The PWM filter, however, had six channels, allowing for configurations with an electrically-biased axial AMB.

During tuning and testing, individual amplifier channels were loaded with a 16mH 1.6Ohm test inductor, composed of eight 2mH toroidal inductors connected in series. These inductors had iron powder cores, resulting in much smaller

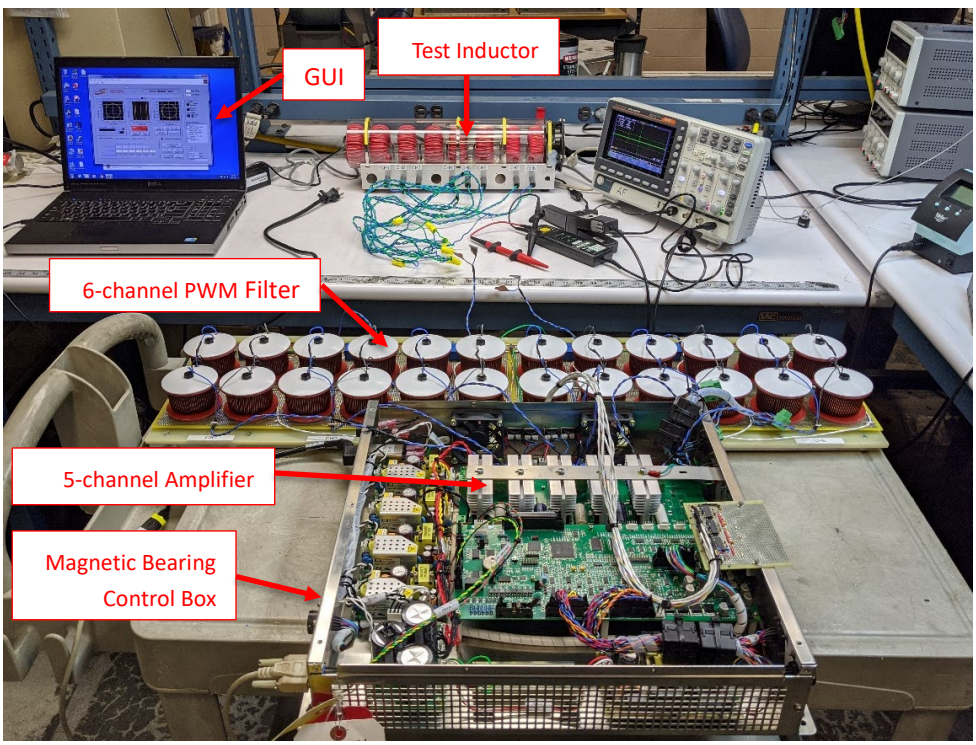

Figure 5. Experimental setup to tune the PWM filter and evaluate its performance on a bench.

eddy-current losses at high frequencies compared to typical AMB actuator coils wound around laminated cores. This represented essentially the worst-case scenario for developing high-frequency ringing on the amplified output induced by harmonics of PWM pulses in the parasitic resonant loops. The ringing would be much smaller if we had used a real AMB actuator with laminated core. A standard AMB control GUI was modified for this test to allow commanding constant duty cycle PWM outputs in addition to the closed-loop operation of the amplifier.

4. Experimental results

4.1. Filter transfer function

Fig. 6 shows overlapped theoretical and measured voltage-to-voltage transfer functions of the proposed filter. The measured transfer function was obtained while outputting 5A DC current, when the maximal PWM harmonic attenuation was expected (-57dB theoretical value at 25kHz). The measured attenuation value at 25kHz in this case was -52.7dB. Because the trap filter inductance values were changing with the output current and the filter was tuned for the resonance to occur close to 25kHz when the output current was 5A, deviations from 5A were leading to lower PWM fundamental harmonic attenuation values. Thus, the attenuation dropped to -36.8dB at 0A and -33.2dB at 10A as shown in Fig. 7 (measured values) – still much higher than the nominal -15dB achievable with the 2nd-order filter only.

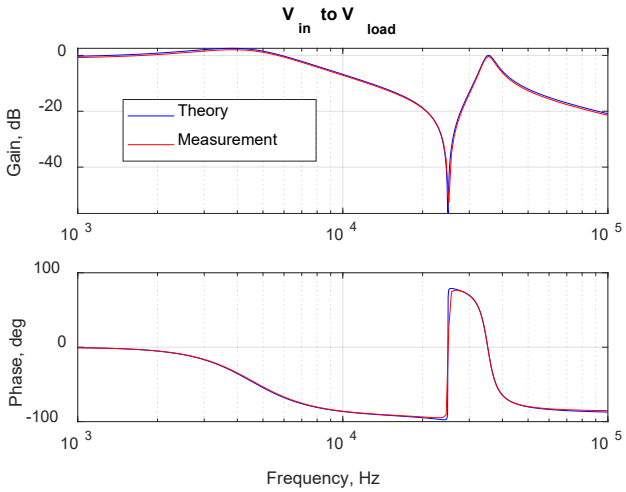

Figure 6. Theoretical and measured with 5A DC output current filter voltage transfer functions.

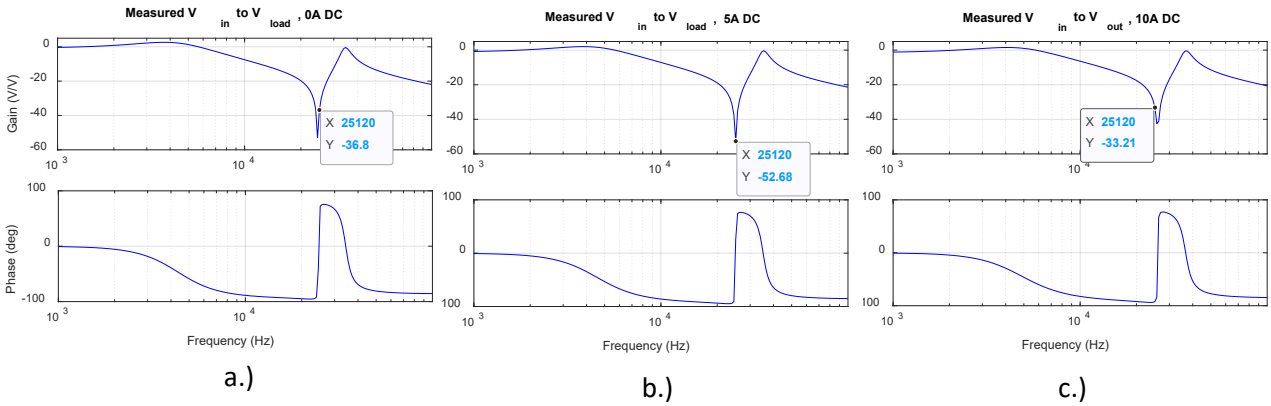

Figure 7. Measured filter voltage transfer functions with 0A DC output current (a), 5A DC (b) and 10A DC (c).

4.2. Open-loop DC-current operation

Figs. 8 and 9 show voltages and currents measured with and without the PWM filter at 5A DC output current level (highest filter effectiveness) and at 10A (lowest filter effectiveness). The amplifier in this measurement was operated in the “open loop” mode, with a DC current level established by manually adjusting the PWM duty cycle. Because the same duty cycle was used with and without the filter, in the latter case the output current was slightly smaller due to the voltage drop on the PWM filter. With both 5A and 10A output currents, the filter effectively suppressed the PWM voltage pulses reducing peak dV/dt by more than 800 times (from 8,360V/μs to approximately 10 V/μs).

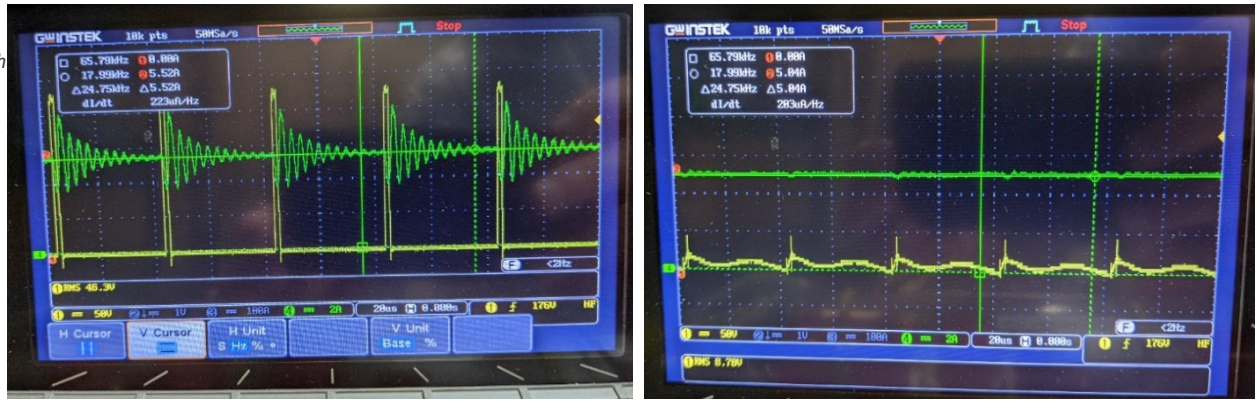

a.) b.)

Figure 8. Measured voltage (yellow) and current (green) on the output of the amplifier without the filter (a) and with the filter (b). The DC output current component was 5.52A without the filter and 5.04A with the filter.

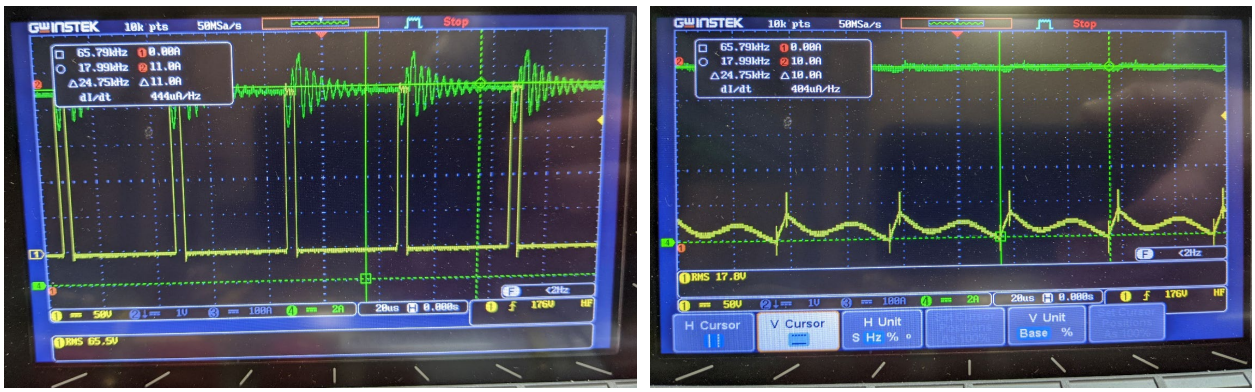

a.) b.)

Figure 9. Measured voltage (yellow) and current (green) on the output of the amplifier without the filter (a) and with the filter (b). The DC output current component was 11.0A without the filter and 10.0A with the filter.

The current waveforms measured without the filter show large oscillations at approximately 250kHz persisting long after the PWM pulses were turned off. Such high-frequency oscillations often occur in parasitic resonant loops on the amplifier output formed by real or parasitic inductances in combination with parasitic capacitances (such as inductor winding capacitances, cable capacitances, amplifier output trace inductances and capacitances, etc.). These oscillations were expected to be unusually large because of low loss level in the test inductors, however the oscillations seen in Figs. 8 and 9 reaching 2A at the peaks are unrealistic, especially if considering that the current probe bandwidth was limited to 100kHz. Most likely these oscillations were electromagnetic noises induced in the scope (or the current probe) by the resonant currents or voltages. Regardless, they disappeared after the introduction of the PWM filter. Fig. 10 shows simulated amplifier output voltage waveforms without the filter (a) and with the filter (b) when outputting 11A DC and

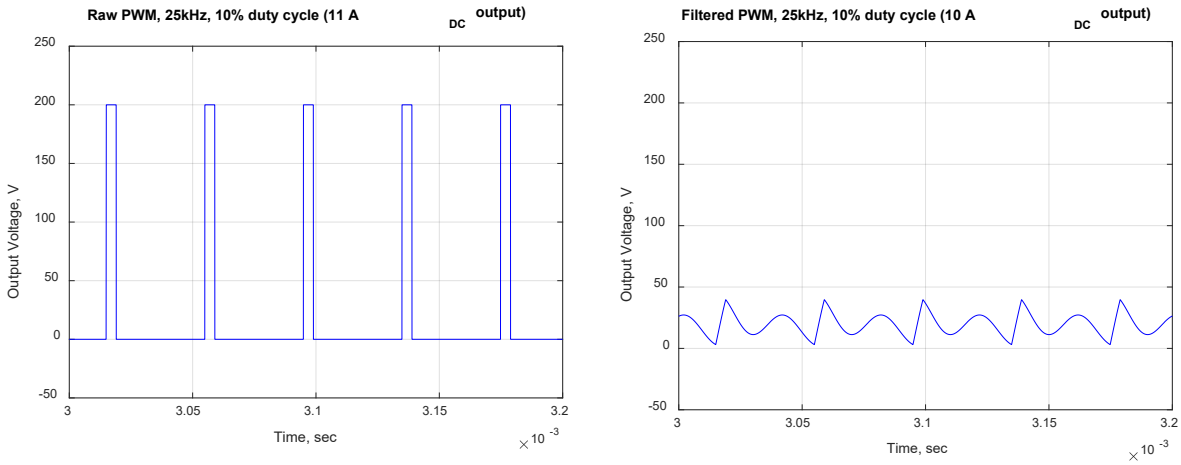

a.) b.)

Figure 10. Simulated amplifier output voltage waveforms without the filter (a) and with the "Trap+LCR" filter (b) when outputting 11A DC and 10A DC respectively. The same 10% duty cycle was used in both cases.

10A DC respectively. The same 10% duty cycle was used in both cases. The simulated filtered voltage waveform Fig. 10b closely resembles the measured ones shown in Fig. 9b.

4.3. Closed-loop AC-current operation

Fig. 11 shows voltages and currents measured after the PWM filter when producing sinusoidal current waveform with 4.4A peak at 100Hz (Fig. 11a) and with 0.8A peak at 1kHz (Fig. 11b) in the closed-loop mode. The current amplitudes at each frequency were limited by the amplifier power supply voltage (200Vdc) combined with the maximum allowable duty cycle (85%). Note that the voltages after the filter are continuous periodical signals rather than trains of PWM pulses and there are no characteristic ripples on the current waveforms. The voltage at 1kHz is nearly sinusoidal, whereas at 100Hz it takes a more complicated shape adjusting to maintain the sinusoidal output current. This is likely because of more pronounced load inductor non-linearity at the larger current achievable at 100Hz.

Fig. 12 shows voltage spectra measured before the PWM filter (a) and after (b) when generating 0.8Apk at 1kHz. The filter does not affect the useful signal at 1kHz, however dramatically reduces PWM sidebands at 13kHz and 16kHz, as well as their harmonics.

Fig. 13 shows simulated amplifier output voltage waveforms when commanding 0.8Apk 1kHz current without the filter (a) with the LCR filter (b) and with the "Trap+LCR" filter (c). Fig. 13c corresponds to the measured waveform shown in Fig. 11b. Clearly the use of the "Trap+LCR" filter (Fig. 13c) results in much cleaner voltage waveform with much smaller ripple compared to the LCR filter alone (Fig. 13b).

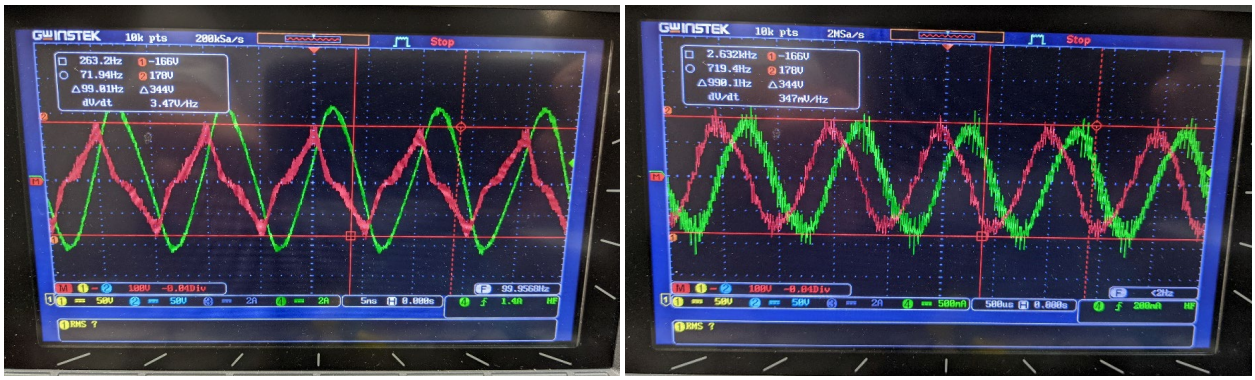

a.) b.)

Figure 11. Measured voltage (red) and current (green) on the output of the amplifier after the filter when producing 4.4Apk 100Hz current (a) and 0.8Apk 1kHz current (b).

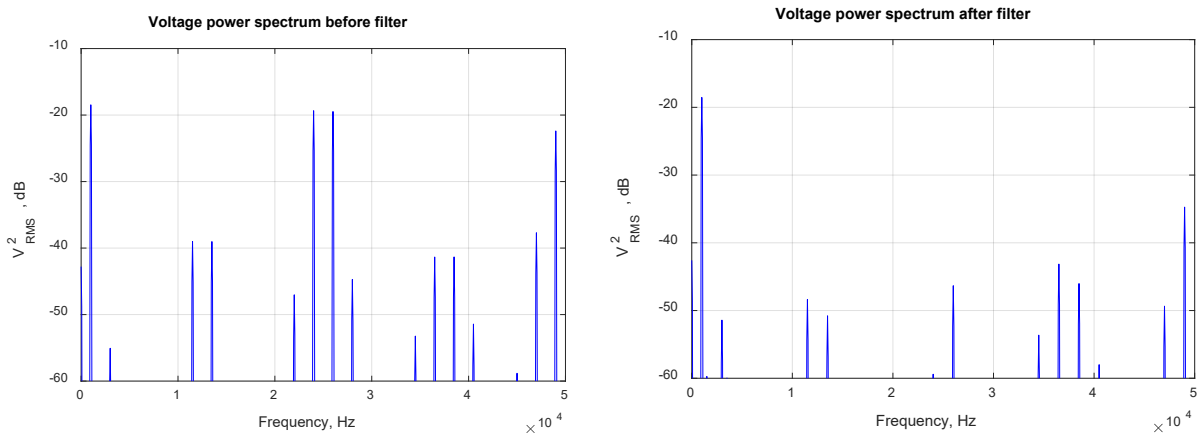

a.) b.)

Figure 12. Measured amplifier output voltage spectra before the filter (a) and after the filter (b) when generating 0.8Apk 1kHz current.

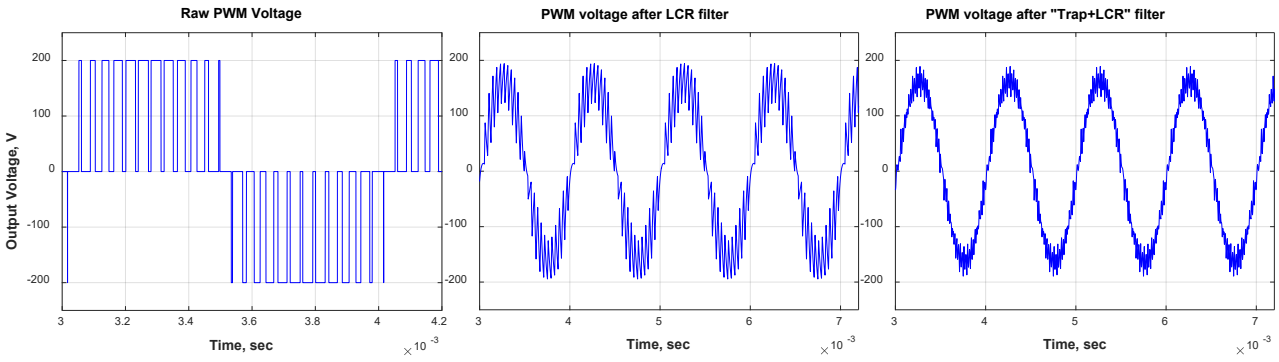

Figure 13. Simulated amplifier output voltage waveforms when commanding 0.8Apk 1kHz current without the filter (a) with the LCR filter (b) and with the "Trap+LCR" filter (c).

4.4. Actuator control over a long cable

Inducing a current in an inductor, such as an AMB actuator winding, using a PWM amplifier becomes challenging when the two are connected by a long cable, which electromagnetic properties cannot be neglected. These properties include specific resistance R_0, inductance L_0 and capacitance C_0 per unit length. For DC voltages and currents, simply more voltage would be needed to drive the same current because of the resistive voltage drop across a cable. The situation becomes much more complicated when high-frequency AC voltages are used, such as PWM pulses. Time-varying electrical signals (voltages and associated currents) propagate along a cable at a specific speed V, which is a fraction of the speed of light in vacuum and is fully defined by the cable parameters L_0 and C_0 (2) (R.K. Moore, 1960).

$$V = \sqrt{\frac{1}{L_0 C_0}} \tag{2}$$

It can be said that all electrical signals travel along a cable as waves with the spatial wavelengths λ inversely dependent on the signal frequencies f as defined by (3). For DC signals $\lambda=\infty$ and this phenomenon can be ignored.

$$\lambda = \frac{V}{f} \tag{3}$$

The level of complications with inducing currents (including DC currents) in an inductor using a PWM amplifier over long cable depends on how close the cable length is to the wavelengths associated with PWM harmonics of significant amplitudes.

1. If the cable length is significantly shorter than the shortest wavelength λ of interest (normally less than ¼ is sufficient), the wave nature of the electrical voltages and currents can be ignored. The cable effect in this case is reduced to adding a lumped cable capacitance in parallel with the inductor. The longer the cable, the bigger the capacitance. When PWM voltage pulses are applied directly to the inductor without a long cable, the current, proportional to an integral of the applied voltage, ends up having a much smoother time waveform than the voltage. In effect, the transfer function from the voltage to the current is an integrator, acting as a low-pass filter. When the cable capacitance is introduced, however, the high-frequency harmonics of the PWM voltage get shorted by this capacitance without reaching the inductor. In addition, the inductor and the cable capacitance form a resonant loop, which may amplify some PWM harmonics.
2. As the cable length approaches the shortest significant spatial wavelength from the PWM spectrum, the voltages and the currents in the cable must be treated as spatial waves and the cable as a "waveguide". Reflected waves may cause the voltages across the amplifier or the inductor to significantly exceed the original amplifier voltage, shortening the life of either the amplifier electronics or the inductor winding, or both. Stationary spatial waves might be also formed with voltage/current peaks and nodes along the cable, which may make AMB control impossible.

In two separate experiments, we used two lines of a 1.2km-long, 3-Phase, 12AWG shielded cable to control currents in either one of the radial channels or the axial channel of a commercial 350kW 15kRPM air compressor. The specific

cable inductance and capacitance between the two lines with the shield ungrounded measured at 2kHz (a low frequency expected to be far below the "waveguide" threshold) were found to be 0.578μH/m and 119pF/m respectively. Using (2) and (3), we estimated that the signal frequency at which the wavelength equals four times the cable length is 25.5kHz – almost exactly the 25kHz amplifier switching frequency and lower than many significant higher-order PWM harmonics.

Fig.14 shows the measured transfer functions from the input current into the 1.2km cable to the output current from the cable into the radial actuator control winding (a) or the axial actuator control winding (b). Note that at high frequencies the currents induced in the actuator windings are not equal to the currents injected into the long cable. This,

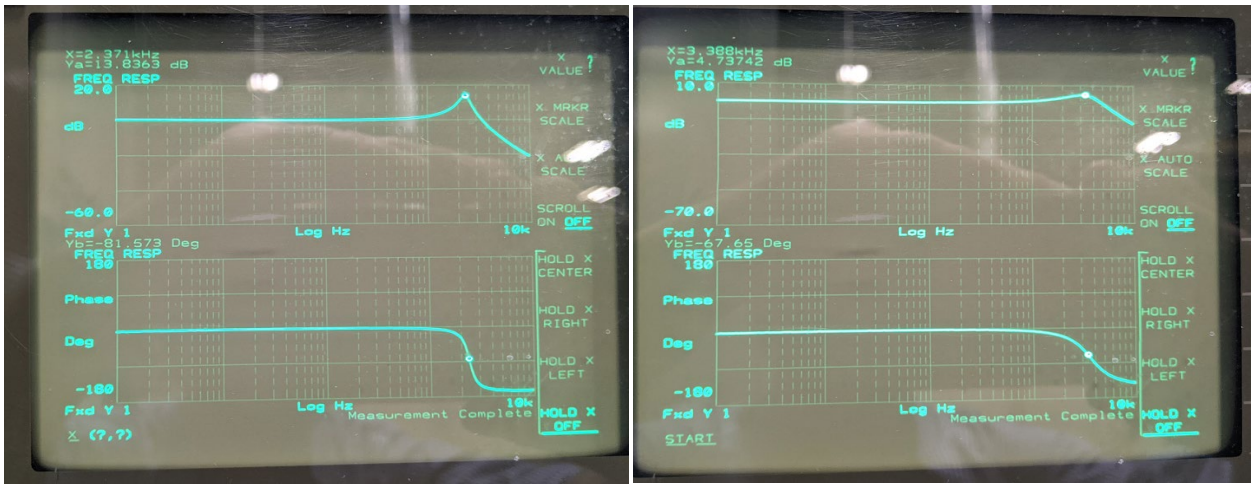

a.) b.)

Figure 14. Measured transfer functions from the input current to the 1.2km cable to the output current from the cable to the radial actuator winding (a) or the axial actuator winding (b).

however, occurs before the "waveguide" threshold and can be explained simply by the presence of the cable capacitance.

To predict the transfer functions such as in Fig. 14 and other effects of a long cable, a finite difference model shown in Fig. 15 was built in LT-Spice. The actuator windings impedances for this model were measured with an LCR meter at several frequencies. Near the resonance at 2.4kHz seen in Fig. 14a, the radial actuator inductance and the effective resistance (accounting for the eddy current losses in the actuator core in addition to the DC resistance) were measured to be 19mH and 43Ohms respectively. For the axial actuator winding near the resonance at 3.4kHz, these parameters were 6.3mH and 80 Ohms. The L/R ratio is much lower for the axial winding because of a non-laminated core.

Fig. 16 shows the current transfer functions as in Fig. 14 predicted using the model shown in Fig. 15 and Table I summarizes measured and predicted resonance frequencies and amplification factors. As can be seen, the analytical predictions match the experimental results reasonably well.

With the PWM filter added, the machine was successfully levitated and spun to full speed with the long cable connected to either the radial or the axial windings.

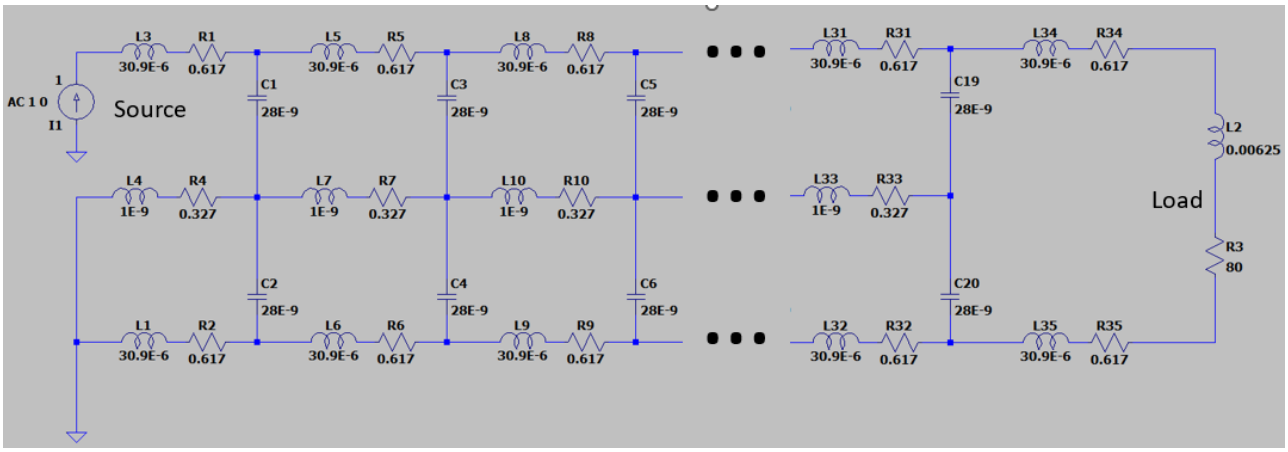

Figure 15. Finite difference LT-Spice model of a long cable with a load.

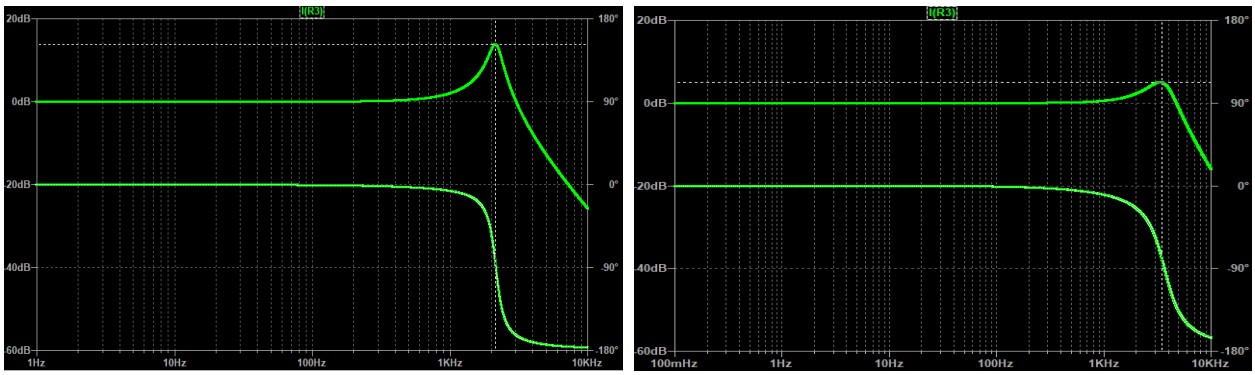

a.) b.)

Figure 16. Transfer functions from the input current to the 1.2km cable to the output current from the cable to the radial actuator winding (a) or the axial actuator winding (b) predicted using the LT-Spice model shown in Fig. 15.

Table I. Comparison of the measured and predicted resonance characteristics on the current over long cable transfer functions.

	f, Hz		Gain, dB	
Bearing	Predicted	Measured	Predicted	Measured
Radial (X2)	2132	2371	13.937	13.836
Axial (Z)	3356	3388	5.116	4.737

5. Conclusions

A combination of a "Trap" filter, utilizing a parallel LC resonant circuit to suppress output current harmonics near the circuit resonance and a conventional 2nd-order LCR filter has been shown very effective in suppressing PWM harmonics in an amplifier with switching frequency close to the upper limit of the required bandwidth. This has been experimentally demonstrated using a PWM amplifier switching at 25kHz with the targeted upper bandwidth limit at 2kHz. The filter has been shown to dramatically reduce switching noises on the output of an amplifier and allowed current control in the radial and axial channels of a commercial 350kW 15kRPM air compressor over 1.2km cable.

References

A. von Jouanne, P. Enjeti and W. Gray (1996) Application issues for PWM adjustable speed AC motor drives. IEEE Industry Applications Magazine, Vol. 2, Issue 5: 10-18.

Essex-Furukawa (2020) Ultrashield Plus and the inverter duty wire market. Available at: https://essexfurukawa.com/wp-content/uploads/2021/10/Essex-Furukawa-White-Paper-UltraShield-Plus-EN.pdf (accessed 11 January 2023).

R.K. Moore (1960) Traveling Wave Engineering. McGraw Hill.

S.W. Smith (1997) The scientist and Engineer's Guide to Digital Signal Processing, 1st edition, California Technical Pub.

Y. Sozer, D. Torrey and S. Reva (2000) New Inverter Output Filter Topology for PWM Motor Drives. IEEE Transactions on Power Electronics, Vol. 15, Issue 6: 911-917.

W. Santiago (2004) Inverter Output Filter Effect on PWM Motor Drives of a Flywheel Energy Storage System. Technical Memorandum TM-2004-213301, NASA, Glenn Research Center, Cleveland, Ohio, USA, September.